Nanoantenna-enhanced absorption in thin infrared detector layers

Michael B Sinclair[1], Larry K Warne[1], Salvatore Campione[1], Michael D Goldflam[1], and David W Peters[1]

***Abstract* – The noise performance of infrared detectors can be improved through utilization of thinner detector layers which reduces thermal and generation-recombination noise currents. However, some infrared detector materials suffer from weak optical absorption and thinning the detector layer can lead to incomplete absorption of the incoming infrared photons which reduces detector quantum efficiency. Here, we show how subwavelength metallic nanoantennas can be used to boost the efficiency of photon absorption for thin detector layers, thereby achieving overall enhanced detector performance.**

1 INTRODUCTION

Several strategies are available to reduce the thermal noise levels of semiconductor infrared detectors. One strategy relies on maximizing the minority carrier lifetime and emphasizes improvement of the detector materials. A second strategy seeks to use thinner detector layers to reduce the overall volume of the detector and thereby reduce the diffusion current due to thermally generated carriers. However, with thinner absorber layers the photon absorption efficiency is decreased, and the overall detector quantum efficiency can suffer. A partial solution to this problem is to fabricate a reflective metal backplane on the back of the detector forming a low quality-factor Fabry-Perot etalon that enhances overall absorption. This solution can be quite effective for specific combinations of detector thickness and absorption coefficient, but does not work well in the general case.

A more general solution to enhancing the absorption of thin infrared detectors can be obtained through the use of a reflective metal backplane in conjunction with a nano antenna (NA) array on the front side of the detector. In this case, the absorption enhancement arises from a combination of resonantly enhanced near-field absorption and impedance matched coupling of external plane waves to the metal-backed detector layer. In this paper, we present a hybrid analytic/numerical approach that allows us to design nanoantenna arrays that achieve optimal absorption of photons in the detector layer. We show that in some spectral ranges capacitive patch arrays are require for good absorption, while in other ranges inductive wire arrays are required. We present numerical simulations of the performance of nanoantenna-enhanced infrared detectors based on realistic thicknesses and optical constants of the detector layer.

2 HYBRID ANALYTIC/NUMERICAL MODEL

Following [1,2], we start with a transmission line analysis of the admittance (Y_{det}) of a metal-backed detector which is given by:

$$Y_{det} = \frac{-i}{\eta_0 \tan(n k_0 d)} \quad (1)$$

Where η_0 is the free-space impedance, n is the complex refractive index of the detector, k_0 the free-space wavevector, and d the detector thickness. When a nanoantenna array is placed on the upper surface, the total input admittance (Y_i) is the sum of the detector admittance and the nanoantenna admittance (Y_{NA}):

$$Y_i = Y_{det} + Y_{NA} \quad (2)$$

Zero reflection, and hence total absorption, will occur if the input admittance is matched to free space [1,2]. Thus, we seek a nanoantenna design that presents an admittance of:

$$Y_{NA} = -Y_{det} + \frac{1}{\eta_0} \quad (3)$$

While it is difficult in general to find an exact solution to Eq. 3, in many cases approximate solutions can be obtained. Our hybrid approach relies on the use of analytic and full-wave electromagnetic simulation to first obtain the detector admittance. Then, full-wave simulations of NA arrays on infinite half-spaces are performed, and the NA array admittances are calculated from the simulated reflectivity. Finally, the design parameters of the NA array are varied, so that an approximate solution to Eq. 3 is obtained at a desired wavelength.

2.1 Detector Admittance

The admittance of the bare detector (with the backplane) can be analytically obtained using Eq. 1. Figure 1 (top panel) shows the analytic admittance (normalized to the free-space admittance) obtained for a 1.2 μm thick detector layer with optical constants that match a strained layer superlattice detector material [3]. Note that the single pass absorption for such a layer is only ~10%.

[1] Sandia National Laboratories, Albuquerque, New Mexico, USA 87185,
e-mail: mbsincl@sandia.gov

Alternatively, the detector/backplane admittance can be obtained by numerically simulating the reflectance of the stack and analytically calculating the admittance from the reflectance. Figure 1 (bottom panel) shows the admittance extracted using this approach. It is evident that there is very good agreement between the analytically and numerically derived admittances. The agreement isn't perfect, however, and the numerically derived admittance suffers from a slight offset of the real admittance to negative values.

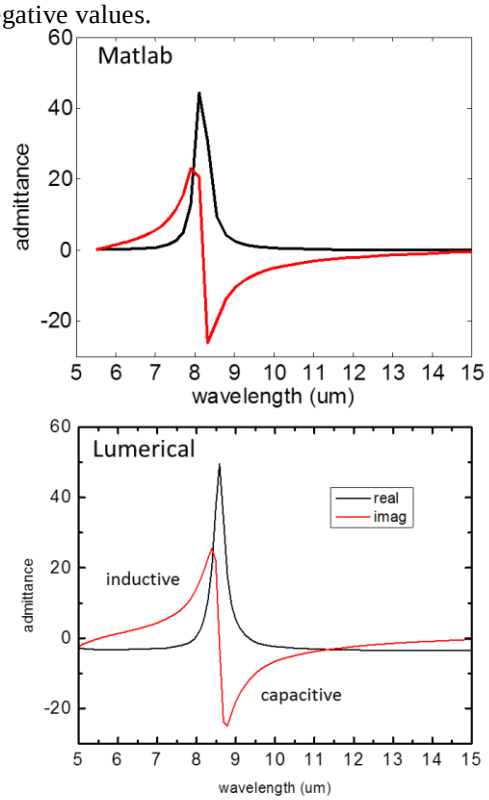

Figure 1: (top) Analytical admittance of the detector/backplane combination obtained using Eq. 1. (bottom) Admittance obtained from the numerically simulated reflectivity.

The real part of the detector/backplane admittance exhibits a prominent peak near 8.5 μm. On the short wavelength side of the peak, the imaginary part of the admittance is positive, indicating inductive behavior. Thus, we anticipate that a capacitive patch array will be required to solve Eq. 3 in this spectral range. In contrast, capacitive behavior is observed on the long wavelength side of the peak, and we anticipate the need for an inductive wire array will be required.

2.1.1 Nanoantenna array admittances

For the remainder of the paper, we will focus on satisfying Eq. 3 on the short wavelength side of the peak in the detector/backplane admittance. In this spectral range we require a capacitive NA patch array. We obtained the admittances of a series of NA patch arrays by first numerically simulating the reflectivity of the NA arrays located on a half space whose real part of the refractive index matched that of the detector layer. Then the admittances were analytically calculated from the simulated reflectivities. For these calculations PEC square patch arrays with duty cycles of 90% were used, and only the overall periodicity was changed. Figure 3 shows the admittances at 10 μm obtained using this procedure (red squares), along with analytically calculated admittance obtained following the formalism of [4]. An excellent agreement is observed between the numerical and analytical admittances.

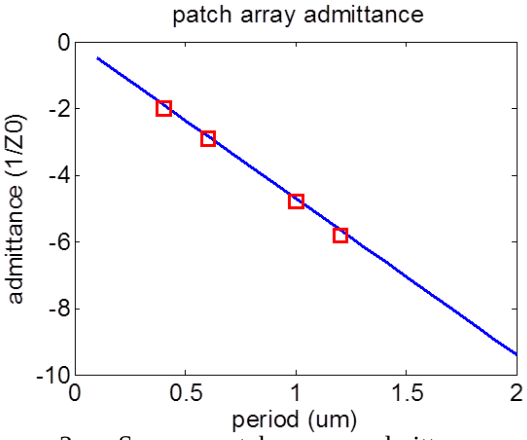

Figure 2. Square patch array admittance as a function of the period obtained using the numerical procedure (red squares). The blue line shows the analytical admittance obtained using the results of [4].

Note that the admittance of the patch arrays becomes increasingly negative as the period is increased. In addition the magnitude of the admittances comparable to the magnitudes observed on the short wavelength side of the peak of the detector/backplane admittance. This suggests that an approximate solution to Eq. 3 may be found in this spectral range using patch arrays.

2.1.2 Optimizing detector absorption

Figure 3 shows the spectral dependence of the 1 um period patch array along with the numerical admittance data shown in Figure 1. The patch array admittance is negative and its magnitude is decreasing with increasing wavelength. Comparison of the imaginary part of the patch array admittance with that of the detector/backplane admittance shows that the two cancel each other near 7.5 μm. The bottom panel of Fig. 3 shows the numerically simulated reflected power (normalized to the incident power) for the full device with the NA array integrated with the detector/backplane stack. A sharp minimum in the reflectivity is observed just above 7 μm, in close proximity to the wavelength where the

imaginary admittances sum to zero. Thus, the addition of the patch array to the device has achieved an approximate solution to Eq. 3.

Note that to ideally satisfy Eq. 3, the real parts of the admittances should sum to 1 (in these normalized units). This is more difficult to achieve than the cancellation of the imaginary parts, but for sufficiently small values of the net real admittance, good absorption efficiency can be obtained. However, as the peak in the real admittance of detector/backplane admittance is approached, the net real part of the admittance becomes very large, and NA-based solutions that lead to low reflectivity cannot be found.

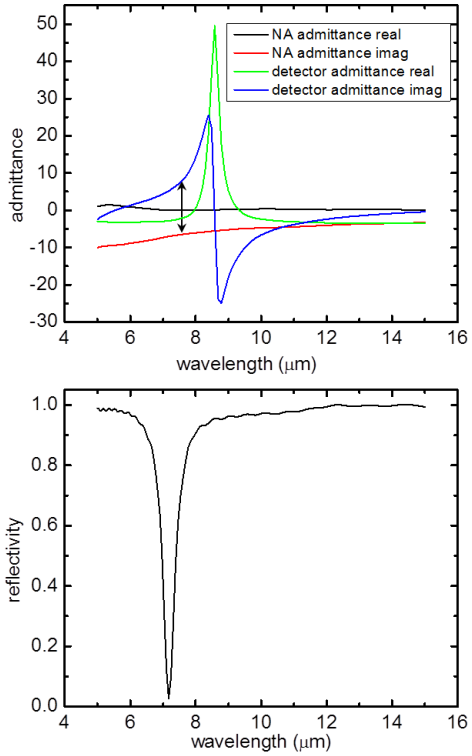

Figure 3: (top) The real and imaginary parts of the admittances of the detector/backplane and the patch array. The arrow indicates the wavelength at which the imaginary parts of the admittances cancel each other. (bottom) The numerically simulated reflectivity of the full device, showing a deep dip in the reflectivity near the wavelength at which the imaginary admittances cancel.

Figure 4 shows the numerically simulated reflectivity for patch arrays of different periods. Once again, a 90% duty cycle, PEC square patch array was used. The wavelength of minimum absorption increases as the period of patch array increases. This is in agreement with the admittances shown in Fig. 1 and Fig. 2. As the wavelength is increased on the short wavelength side of the peak in Fig. 1, the imaginary admittance is positive and increasing. Figure 2 shows that the patch array admittance is negative and increasing in magnitude as the period is increased. Thus, we expect that the cancellation point should shift to longer wavelengths as the period increases. Note also, that the minimum of the reflectivity is also increasing with the array period. This is due to the large value of the net real part of the admittance as the admittance peak is approached.

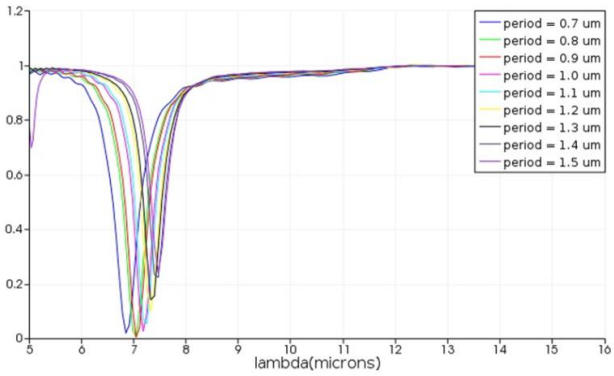

Figure 4. The numerically simulated reflectivity for the integrated NA/detector/backplane device as a function of the patch array period.

3 CONCLUSION

In conclusion, we have presented a hybrid analytic/numerical procedure to aid the design of nanoantenna arrays to achieve efficient photon absorption in thin infrared detectors. We showed that on the short wavelength side of the detector/backplane admittance peak, a capacitive patch array can be used to approximately satisfy Eq. 3 and obtain good absorption efficiency. A similar analysis on the long wavelength side of the admittance peak shows that inductive wire arrays can be used to achieve good absorption.

Acknowledgments

This research was supported by the Laboratory Directed Research and Development program at Sandia National Laboratories. Sandia National Laboratories is a multimission laboratory managed and operated by National Technology and Engineering Solutions of Sandia, LLC., a wholly owned subsidiary of Honeywell International, Inc., for the U.S. Department of Energy's National Nuclear Security Administration under contract DE-NA-0003525.

References

[1] S. Tretyakov, "Thin absorbers: operational principles and various realizations", IEEE Electromagnetic Compatibility Magazine, 5, 61, 2016.

[2] Y. Ra'di, C. R. Simovski, and S. A. Tretyakov, "Thin Perfect Absorbers for Electromagnetic Waves: Theory, Design, and Realizations" Phys. Rev. Applied **3**, 037001 (2015)
[3] S. Tretyakov, "Analytical Modeling in Applied Electromagnetics", London, UK: Artech House (2003).
[4] Goldflam, M. D., E. A. Kadlec, B. V. Olson, J. F. Klem, S. D. Hawkins, S. Parameswaran, W. T. Coon, G. A. Keeler, T. R. Fortune, A. Tauke-Pedretti, J. R. Wendt, E. A. Shaner, P. S. Davids, J. K. Kim, and D. W. Peters, "Enhanced infrared detectors using resonant structures combined with thin type-II superlattice absorbers," Appl. Phys. Lett., **109**, 251103, 2016